N O T I C E

THIS DOCUMENT HAS BEEN REPRODUCED FROM MICROFICHE. ALTHOUGH IT IS RECOGNIZED THAT CERTAIN PORTIONS ARE ILLEGIBLE, IT IS BEING RELEASED IN THE INTEREST OF MAKING AVAILABLE AS MUCH INFORMATION AS POSSIBLE

Mountain Winds - Revisited

Eugene Isaacson , Gideon Zwas

Abstract

The prediction of extremely high wind speeds, at ground
level on the downstream side of a mountain range, is possible
by solving the initial value problem for a two-layered nonlinear
"shallow-water" model of the atmosphere. Three different
numerical methods are described to find the solutions which may
involve shocks: (i) the vonNeumann-Richtmyer artificial viscosity
method, (ii) a _ltering scheme, and (iii) a hybrid method.

1.   Introduction

Occasionally, when air is crossing at moderate speed
over the top of a mountain range, extremely high wind speeds
will develop at ground level on the lee (downstream) side
[5].   Simple one-layered [4] and two-layered [3]
nonlinear "shallow-water" models of the troposphere were
designed and used to study this phenomenon. For a large
class of initial values, such asymmetric steady flows were
found to develop quickly in time, even when the mountain
is taken to be a symmetric parabolic arc. The numerical
method used in [3] to produce the steady-state solutions
made use of a von Neumann and Richtmyer [6]   pseudo-viscosity
term, which was "switched on" in regions of "compression"
only. This artificial viscosity method was needed to suppress
the post-shock oscillations that would have otherwise
developed in the levels and velocities of the two-layered
model. Since these flows often contained stationary shocks
on the lee side of the mountain, such post shock oscillations
would have seriously masked the true nature of the steady
states. In   [3], the use of this "compression switch"
prevented the application of the artificial viscosity term
near the upstream base of the mountain, for a physically
realizable subset of initial values. In these cases, spurious
oscillations developed on the upstream side of the mountain
and continued downstream, so that the detection of a steady state
flow over the mountain was prevented.

The present work verifies that indeed for all initial values of physical interest, steady states do develop over the mountain in the two-layered model. We therefore believe that the shallow-water models can be used to forecast such ground level strong winds on the lee side of mountains.

The correct steady state solutions are found independently by the use of three different numerical methods: (i) by eliminating the compression switch, i.e., so that the pseudo-viscosity term is always present; (ii) by using a filtering scheme; (iii) by using a hybrid scheme. The numerical results obtained from these three methods have close agreement. In section 2, we describe the differential equations of the two-layered model, the parameters that characterize the initial values, and the nature of the physically relevant solutions. In section 3, we describe the three numerical methods and comment on their advantages and disadvantages.

2. Differential equations, initial data, and solutions.

The time dependent, two-layered, long wave, incompressible fluid model, for flow in a plane perpendicular to the earth and to the mountain ridge, is governed by the partial differential equation system [3], for the vector $w = w(x,t)$:

(1)
$$w_t + G_x + K = 0 ,$$

where

$$w \equiv \begin{pmatrix} m \\ \phi \\ m' \\ \phi' \end{pmatrix} , \qquad G \equiv \begin{pmatrix} \frac{m^2}{\phi} + \frac{g\phi^2}{2} \\ m \\ \frac{m'^2}{\phi'} + \frac{g\phi'^2}{2} \\ m' \end{pmatrix}$$

$$K \equiv g \begin{pmatrix} \phi(r\phi' + H)_x \\ 0 \\ \phi'(\phi + H)_x \\ 0 \end{pmatrix}$$

We have chosen u and ϕ to represent the horizontal velocity and the depth respectively of the lower fluid layer, and the same quantities primed (u',ϕ') to represent velocity and depth for the upper layer (see Figure 1). Since we will be computing flows that have shocks, it is appropriate to work with

$$m \equiv u\phi , \quad m' \equiv u'\phi' ,$$

representing the momentum per unit length (and density), in
the lower and upper layers respectively. The constant quantity,
r (r $\leq$ 1), is the ratio ρ_1/ρ of the densities ρ_1 of the
upper layer and ρ of the lower layer, g denotes the
gravitational constant, while H = H(x) is the formula represent-
ing the height, above some datum, of the ground. We remark
that [3] treats also the case of a three-layered model,
in which the highest layer is passive, by means of a quite
similar system of equations that incorporates a constant,
s; namely, the ratio of the densities of the topmost and bottom-
most layers and that deals solely with the same dependent
variables u, ϕ, u', and ϕ'. It would have been simple to
formulate the corresponding difference schemes for this
three-layered model, since it is governed again by a system
of four, first order, partial differential equations with
different constants in the coefficients.

As was observed in [3], the system (1) is hyperbolic,
when its four characteristic speeds, dx/dt = μ , are
real and distinct; namely, when the roots, $\mu = \mu_j(x,t)$ for
j = 1,2,3,4, of the following quartic equation are real and
distinct, $\mu_1 < \mu_2 < \mu_3 < \mu_4$;

(2) $[(u - \mu)^2 - g\phi][(u' - \mu)^2 - g\phi'] - rg^2\phi \phi' = 0$.

We expect that the initial value problem for (1) is well posed,
when the four roots are real and distinct for the initial data.

The family of steady solutions (i.e., time independent) of (1) is found in [3] by studying the limit as $t \to \infty$ of the numerical solutions of initial value problems for suitable choices of impulsive initial data. That is, the initial velocities $u(x,0)$ and $u'(x,0)$ are set to be constant and the tops of the two layers are initially chosen to be horizontal. It was found by doing many subsidiary numerical calculations with such data, that all of the qualitative features of the steady state solutions were exhibited by the solutions that arose from a special choice of the parameters that represent the initial data. That is, when the mountain profile is a simple parabolic arc

$$(3) \qquad H(x) \equiv \begin{cases} h(x) , & |x| \le a , \\ 0 , & |x| > a , \end{cases}$$

where

$$(4) \qquad h(x) = H_c\left(1 - \frac{x^2}{a^2}\right);$$

simply assume that the initial velocities are constant and equal, say

$$(5) \qquad u(x,0) = u'(x,0) = u_{-\infty} ;$$

and suppose that the initially constant height of the lower layer, $\phi(x,0) + H(x)$, equals the initially constant depth of the upper layer, $\phi'(x,0)$:

(6) $\phi(x,0) + H(x) = \phi'(x,0) = \phi_{-\infty}$;

and finally select a value for r. It then is appropriate to consider the two dimensionless parameters

(7) $F_0 \equiv \dfrac{u_{-\infty}}{\sqrt{g\phi_{-\omega}}}$, and $M_c \equiv \dfrac{H_c}{\phi_{-\infty}}$

as determining the initial data.

In [3], the (F_0, M_c) plane is divided into regions, each producing a different kind of limiting solution as $t \to \infty$, from the corresponding choice of initial data. In particular, we reproduce a figure of [3] as Figure 2, and observe that r = 0.8 and regions [*] A, B and B' are the ones that correspond to physically realizable velocities in the atmosphere. We note that this model should not be used to make calculations for data in region A. For region A, it would be appropriate to use the more conventional linearized theory in two spatial dimensions, to describe the sinusoidal lee waves that occur in nature. On the other hand, it is the development of a high lee side velocity in the steady asymmetric solutions for regions B and B', that leads us to recommend the use of this nonlinear model to describe and predict the strong wind phenomena on the downstream side of a mountain range.

In [3], a steady solution was approached for initial data in region B. The steady solution was asymmetric over

---

[*] We have been informed by D. Houghton that S. C. Mehrotra has communicated the fact that when the depth of the upper layer is much larger than the depth of the lower layer, then the size of region A is much smaller.

the mountain top. This asymmetry was possible since $\mu_3 = 0$, at the top of the mountain where $H_x = 0$. A schematic drawing of the resulting flow is taken from a figure of [3] and reproduced as Figure 3 here. The characteristic curves $dx/dt = \mu_i$ are said to be external for $i = 1,4$ and internal for $i = 2,3$. A confluence of characteristics with $i = 1$ (or with $i = 4$) is said to produce an external shock; a region having straight characteristics for $i = 2$ (or for $i = 3$) is said to be an internal rarefaction wave, while if $i = 1$ or 4 the wave is called external. On the lee side of the mountain, μ_3 also approaches zero at a point on the mountain side. This caused a confluence of the internal characteristics which accompany the stationary shock, that is thus called internal and which is located on the mountain side.

Note that in a steady state solution the conservation of mass in the lower layer, described by the second component of equation (1), implies that $\phi u \equiv m = $ constant. Hence, where the depth ϕ decreases, the velocity u must increase. Observe that this situation occurs on the lee side of the mountain, and can explain how the high velocities develop there.

But we remark that the numerical method of [3] produced a spurious solution for data in region B'; namely, the initially impulsive motion for B' did not seem to tend to a steady state over the mountain. In fact the curve separating regions B and B' was determined by numerical

experiments. That is, for region B', numerically spurious waves were continuously generated on the upstream side of the mountain and these waves traveled both up and downstream, thus preventing the development of a steady motion. See typical Figures 4a and 4b for computer plots of the heights of the two air layers at two different times as found by the method of [3].. On the other hand, when using any of the three different numerical methods described in the next section, the spurious waves do not appear for data in region B'. See Figures 5, 6, and 7 that show the solutions obtained by these methods, for the same data in region B'.

We find that for initial data in region B', the characteristic $\mu_2 = 0$ at x = -a, i.e. at the upstream edge of the mountain. (Since the flow is not compressing here, the pseudo-viscosity term was not switched on in [3]. But, as is well known the Lax-Wendroff scheme is not dissipative where a characteristic is stationary, so that the large force term H_x , caused disturbances to begin at x = - a and move into the flow. This error growth could be minimized by using a much smaller spatial interval, and could be lessened somewhat by introducing a smooth transition region between the flat earth and the parabolic mountain edge.) We further observe that the flow is symmetric over the top of the mountain, until a weak stationary shock forms on the lee mountainside, with the accompanying confluence of the characteristics dx/dt = μ_2. A stronger downstream shock is also formed with the confluence

of the μ_2 characteristics. This stronger shock is stationary
on the mountain side for some range of initial parameters
in B', but in the remainder of the B' region this strong shock
keeps moving slowly downstream.

In summary, we find that for any data in regions B and B',
the wind speed near the ground on the lee side is much higher
than on the upstream side, in the steady state solution that
rapidly develops.

3. Numerical Methods

(1) Pseudo-Viscosity

The pseudo-viscosity method [6] devised by von Neumann and Richtmyer, was applied to the Lax-Wendroff (L-W) scheme in [3]. Here we use W to represent the discrete approximation to the solution w of equation (1). Symbolically we set

$$(8) \quad W(t + \Delta t) = W(t) + \Delta t\, W_t(t) + \frac{(\Delta t)^2}{2} W_{tt}(t) \;,$$

where the time derivatives are to be replaced by spatial derivatives obtained from equation (1), and then the first and second order spatial derivatives are to be replaced by suitably centered difference approximations. Therefore

$$(9) \quad W(t + \Delta t) = W - \Delta t(G_x + K) + \frac{(\Delta t)^2}{2} \left\{ [A(G_x + K)]_x + K_t \right\} \;,$$

where $A \equiv \partial G / \partial w$ is the Jacobian matrix and where all terms on the right-hand side of (9) are to be evaluated at $W(t)$, with

$$K_t \equiv g \begin{Bmatrix} m_x(r\phi' + H)_x + r\phi m'_{xx} \\ 0 \\ m'_x(\phi + H)_x + \phi' m_{xx} \\ 0 \end{Bmatrix}$$

The difference expression for (9) is

(10) $W_j^{n+1} = W_j^n - \frac{\lambda}{2} [\Delta_0 G_j^n + 2\Delta x\, K_j^n]$

$$+ \frac{\lambda^2}{2} \left[A_{j+\frac{1}{2}}^n (\Delta_+ G_j^n + \Delta x\, K_{j+\frac{1}{2}}^n) - A_{j-\frac{1}{2}}^n (\Delta_+ G_{j-1}^n + \Delta x\, K_{j-\frac{1}{2}}^n) \right]$$

$$+ \frac{\lambda^2}{2} (\Delta x)^2 (K_t)_j^n$$

where for any function $\psi(x,t)$, we define for integer j, $\psi_j^n \equiv \psi(x_j, t_n)$, $\lambda = \Delta t / \Delta x$, $x_j = j\, \Delta x$, $t_n = n\, \Delta t$, with Δx and Δt representing the space and time increments used in the difference scheme; the operators Δ_0 and Δ_+ are defined by

$$\Delta_0 f = f_{j+1} - f_{j-1} ,$$

$$\Delta_+ f_j = f_{j+1} - f_j ;$$

while

$$\Delta x\, K_{j+\frac{1}{2}} \equiv g \begin{pmatrix} \phi_{j+\frac{1}{2}} \Delta_+ (r\phi_j' + H_j) \\ 0 \\ \phi_{j+\frac{1}{2}}' \Delta_+ (\phi_j + H_j) \\ 0 \end{pmatrix}$$

with the convention for $f \equiv \phi$, ϕ', or A,

$$f_{j+\frac{1}{2}} \equiv \frac{1}{2} (f_{j+1} + f_j) ,$$

and define $K_{j-\frac{1}{2}}$ and $f_{j-\frac{1}{2}}$ by replacing j by $j-1$; furthermore,

$$2 \, \Delta x \, K_j \equiv \frac{g}{2} \left[\begin{array}{c} (\phi_{j+1} + \phi_{j-1}) \, \Delta_0 (r\phi_j' + H_j) \\ 0 \\ (\phi_{j+1}' + \phi_{j-1}') \, \Delta_0 (\phi_j + H_j) \\ 0 \end{array} \right] \quad ,$$

and finally,

$$(\Delta x)^2 (K_t)_j \equiv \frac{g}{4} \left[\begin{array}{c} (\Delta_0 m_j) [\Delta_0 (r\phi_j' + H_j)] + 2r(\phi_{j+1} + \phi_{j-1}) \Delta_+ (\Delta_+ m_{j-1}')] \\ 0 \\ (\Delta_0 m_j') [\Delta_0 (\phi_j + H_j)] + 2(\phi_{j+1}' + \phi_{j-1}') \Delta_+ (\Delta_+ m_{j-1}')] \\ 0 \end{array} \right]$$

The Lax-Wendroff scheme (9) is modified by the introduction of a pseudo-viscosity expression B in the Δt term as follows:

$$(11) \quad W(t+\Delta t) = W - \Delta t [(G + B)_x + K] + \frac{(\Delta t)^2}{2} \{ [A(G_x + K)]_x + K_t \}$$

where

$$B \equiv \alpha (\Delta x)^2 \left[\begin{array}{c} \phi u_x |u_x| \\ 0 \\ \phi' u_x' |u_x'| \\ 0 \end{array} \right]$$

Here $(\Delta x) B_x$ is replaced by $(B_{j+\frac{1}{2}} - B_{j-\frac{1}{2}})$, with $B_{j\pm\frac{1}{2}}$ defined in a manner analogous to the way $K_{j\pm\frac{1}{2}}$ are defined. In [3], $\alpha \neq 0$ at any mesh point j where either $u_x \leq 0$ or $u_x' \leq 0$; while, if neither inequality holds, then $\alpha = 0$.

This is the compression switch, which is tested by checking centered velocity differences for each layer. But, as explained in section 2, we found that it is desirable to keep $\alpha \neq 0$ everywhere. For the parabolic mountain the optimum range of α is (1, 2.5). Note that the introduction of the dimensionless parameters in (7) for velocity and length implies that a dimensionless time unit is also introduced consistently by introducing $\sqrt{\phi_{-\infty}/g}$ as the unit of time. In this way, it is easy to verify that the dimensionless gravitational constant $g = 1$. Our calculations are performed with a = 1 and with periodic boundary conditions imposed at $x = \pm L$, where $L = 50$ and $\Delta x = \frac{1}{20}$. The impulsive motion could be computed as long as the periodicity condition does not produce interference with the flow near the mountain. Occasionally, $L = 100$ was used in order to prevent such interference effects. The Courant-Friedrichs-Lewy (CFL) stability condition for (L-W) is $\lambda(\max_j |\mu_j|) \leq 1$. In the pseudo-viscosity scheme, it is sometimes necessary to restrict the time step further, in order to maintain the stability of the scheme.

(ii) Filter

The filter was developed in [1] to facilitate the calculation of one and two dimensional aerodynamical flows with shocks. The filter may be inserted easily into an existing program. For example, if the basic Lax-Wendroff scheme (9), (10) is represented in the operator form

$$(12) \qquad W_j^{n+1} = T W_j^n \ ,$$

then the filter scheme has the form

$$(13) \qquad V_j^{n+1} = T W_j^n \ ,$$

$$(14) \quad W_j^{n+1} = V_j^{n+1} + \frac{1}{4} [\theta_{j+\frac{1}{2}}^n (V_{j+1}^{n+1} - V_j^{n+1}) - \theta_{j-\frac{1}{2}}^n (V_j^{n+1} - V_{j-1}^{n+1})]$$

That is,

$$W_j^{n+1} = V_j^{n+1} + \frac{1}{4} [\theta_{j+\frac{1}{2}}^n \Delta_+ V_j^{n+1} - \theta_{j-\frac{1}{2}}^n \Delta_+ V_{j-1}^{n+1}] \ .$$

Note that if $\theta \equiv 1$, then the filter is called a Shuman filter, and it smooths short wave length oscillations in the solution everywhere. Here, we employ θ as a switch; namely,

$$(15) \qquad \theta_{j+\frac{1}{2}} = \beta \left[\frac{|z_{j+1} - z_j|}{\max\limits_{\ell} |z_{\ell+1} - z_\ell|} \right]^m \ ,$$

where z is any dependent function that is a good "sensor" of large gradients, for example, $z \equiv u$ the velocity in the lower layer; m is one less than the order of accuracy of the operator T in (12), that is $m = 1$; and the constant β lies in the range $(0,2)$. For this range of β [1] showed that for constant coefficients, the scheme (13), (14) is stable if (12) is stable. In practice, we found that for the two-layered flow the constant β should be chosen in the range $(0.25, 0.75)$, with the additional proviso that $\beta \equiv 0$

at any times when the flow is so smooth that

$$\max_j |\Delta_+ u_j| < \frac{\Delta x}{2} .$$

(iii) Hybrid

Hybrid schemes were developed and analyzed in [2] to facilitate the calculation of flows with shocks. The idea is to use an operator that "interpolates" between two operators: a first order accurate operator that provides mono- tonic, and slightly diffused shock profiles; and a second order accurate operator. Here the interpolation is done with a switch analogous to (15) which is sensitive to large gradients in the solution. Let the first order Lax-Friedrichs scheme be denoted by

(16)
$$W_j^{n+1} = S\ W_j^n$$

where

$$S\ W_j^n = \frac{1}{2}\ (W_{j+1}^n + W_{j-1}^n) + \Delta t\ W_t^n$$

$$= \frac{1}{2}\ (W_{j+1}^n + W_{j-1}^n) - \Delta t (G_x + K)_j^n$$

$$= \frac{1}{2}\ (W_{j+1}^n + W_{j-1}^n) - \frac{\lambda}{2}\ [\Delta_0 G_j^n + 2\ \Delta x\ K_j^n]$$

$$= W_j^n + \frac{1}{2}\ (\Delta_+ W_j^n - \Delta_+ W_{j-1}^n) - \frac{\lambda}{2}\ [\Delta_0 G_j^n + 2\ \Delta x\ K_j^n] .$$

Then the hybrid scheme is suggested by the form

$$W_j^{n+1} = (\theta S + (1-\theta) T) W_j^n .$$

That is,

$$(17) \quad W_j^{n+1} = W_j^n - \frac{\lambda}{2} [\Delta_0 G_j^n + 2 \Delta x K_j^n] + \frac{1}{2} [\theta_{j+\frac{1}{2}}^n \Delta_+ W_j^n - \theta_{j-\frac{1}{2}}^n \Delta_+ W_{j-1}^n]$$

$$+ \frac{\lambda^2}{2} \left[(1-\theta_{j+\frac{1}{2}}^n) A_{j+\frac{1}{2}}^n (\Delta_+ G_j^n + \Delta x K_{j+\frac{1}{2}}^n) \right.$$

$$\left. - (1-\theta_{j-\frac{1}{2}}^n) A_{j-\frac{1}{2}}^n (\Delta_+ G_{j-1}^n + \Delta x K_{j-\frac{1}{2}}^n) + (1-\theta_j^n)(K_t)_j^n \right] ,$$

where

$$\theta_j^n \equiv \frac{1}{2} (\theta_{j+\frac{1}{2}}^n + \theta_{j-\frac{1}{2}}^n) .$$

As shown in [1] and [2], the filtering and hybrid schemes are stable when they use the CFL condition appropriate to the basic operators S and T. But, the pseudo-viscosity scheme may impose a further restriction on the time step (see [6]). In fact, we find that when a strong shock occurs in the two-layered model, it is sometimes necessary to reduce the time step by a factor of 1/2 , to achieve stability for the artificial viscosity scheme.

In conclusion, we exhibit a calculation of the flow over a profile of the Rocky Mountains made with the filtering method (14) where the constant $\beta = 0.4$. The topographical

cross-section is the one used in [3] with initial data given on p. 45. The constant $\phi_{-\infty}$ = 9,000 ft., and represents the initial depth of the lower layer which lies above the 5,000 foot elevation of the plains east of Denver, while 21,000 feet is the initial depth of the upper layer. The initial velocities are u = 18 m/sec , and u' = 28 m/sec , while r = 0.946 is the ratio of the densities of the two layers. Figure 8 shows the position of the tops of the two layers after 3750 time steps, which represents about 5 hours and 25 minutes of elapsed time. The relatively steady flow now exhibits the large increase in velocity in the lower layer on the lee side of the mountain range, and a "stationary shock" that is near the base of the mountain. The mountain profile is the lowest curve drawn. Here the 340 km topography is taken for a slice from Denver, at x = 1, west to the Colorado border at x = -4. The plains to the east of Denver are taken to be level at 5000 ft. above sea level, and the slope to the west of the Utah-Colorado border is simulated as being constant until the height of 5000 ft. is reached at x = - 6.5, and further west the ground remains flat. Zero on the Y axis corresponds to 5000 ft. above sea level, while 3.32 on the Y axis corresponds to 35,000 ft. above sea level.

Bibliography

[1]   Harten, A. and G. Zwas, "Switched Shuman Filters for
       Shock Calculations, Eng. Math., v. 6, 1972, 207-216.

[2]   Harten, A. and G. Zwas, "Self Adjusting Hybrid Schemes
       for Shock Calculations," J. Comp. Physics, v. 9, 1972,
       568-583.

[3]   Houghton, D. and E. Isaacson, "Mountain Winds,"
       Studies in Num. Analysis 2, SIAM, 1968, 21-52.

[4]   Houghton, D. and A. Kasahara, "Nonlinear Shallow Fluid
       Flow over an Isolated Ridge," Comm. Pure Appl. Math.,
       v. 21, 1968, 1-23.

[5]   Julian, L. T. and Julian, P. R., "Boulder's Winds,"
       Weatherwise, v. 22, 1969, 108-112.

Richtmyer's inspiring work continues to be most often
quoted. We are happy to acknowledge our indebtedness and
extend birthday greetings.

[6]   Richtmyer, R. and K. W. Morton, "Difference Methods for
       Initial-Value Problems," Interscience-Wiley, 1967.

Many studies have been made of strong mountain winds.
The following representative works consider two space dimensional
models of the flow in a vertical plane. They are concerned
with giving a description that is valid throughout the plane
and not just near the ground. In particular, some interesting

phenomena that occur up into the lower stratosphere are analyzed.

Klemp, J. B., and D. K. Lilly,   "Numerical Simulation of
Hydrostatic Mountain Waves," J. Atmos. Sci., v. 35,
1978, 78-107.

Lilly, D. K., "A Severe Downslope Windstorm and Aircraft
Turbulence Event Induced by a Mountain Wave,"
J. Atmos. Sci. v. 35, 1978, 59-77.

Peltier, W. R. and T. L. Clark, "The Evolution and Stability
of Finite-Amplitude Mountain Waves. Part II: Surface
Wave Drag and Severe Downslope Windstorms,"
J. Atmos. Sci., v. 36, 1979, 1498-1529.

CAPTIONS

Figure

1   Schematic drawing of a two-layered atmosphere over a bump.

2   Regions in the (M_c, F_0) plane of initial data, for $r = 0.8$. The regions of physically realistic initial data are A, B, and B'. The shallow water model is appropriate for data in regions B and B'.

3   Schematic drawing of a flow that results from initial data in region B. The curves plotted show H, $\phi + H$, and $\phi' + \phi + H$ as functions of x. The flow is steady near the mountain.

4a, b   Computer plots of solution obtained by the method in [3], for initial data, $F_0 = 0.25$, $M_c = 0.6$, $r = 0.8$, in region B'. Note spurious wavelike motion that spreads from upstream edge of mountain (a) at 1500 time steps and (b) at 1750 time steps. Here artificial viscosity coefficient $\alpha = 2$, $a = 1$, $\Delta x = 0.05$, and $\lambda \leq 0.85$ (of the maximum permissible CFL ratio). Δt varies in time. Dimensionless time T is printed.

5   For the initial data and parameter values used in Fig. 4, computer plot at 1750 time steps of the solution obtained with the pseudo-viscosity method (i.e. artificial viscosity term used everywhere). Flow is steady near the mountain.

6   For the initial data used in Fig. 4 and $\beta = 0.5$, computer plot at 1750 time steps of solution obtained with the filtering method. Flow is steady near the mountain.

7   For the initial data used in Fig. 4 and $\beta = 0.25$,
    computer plot at 1750 time steps of solution obtained
    with the hybrid method. Flow is steady near the
    mountain.

8   Flow over the Rocky Mountains after 3750 time steps,
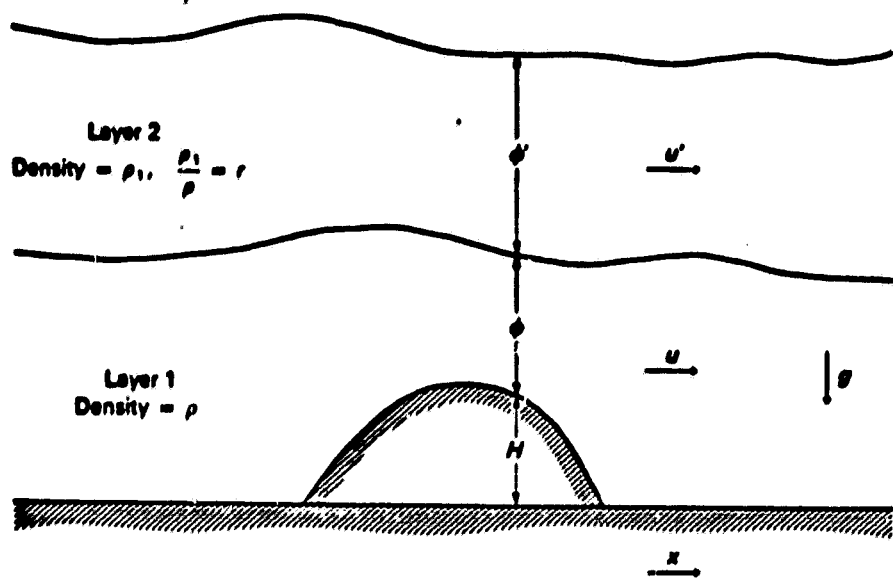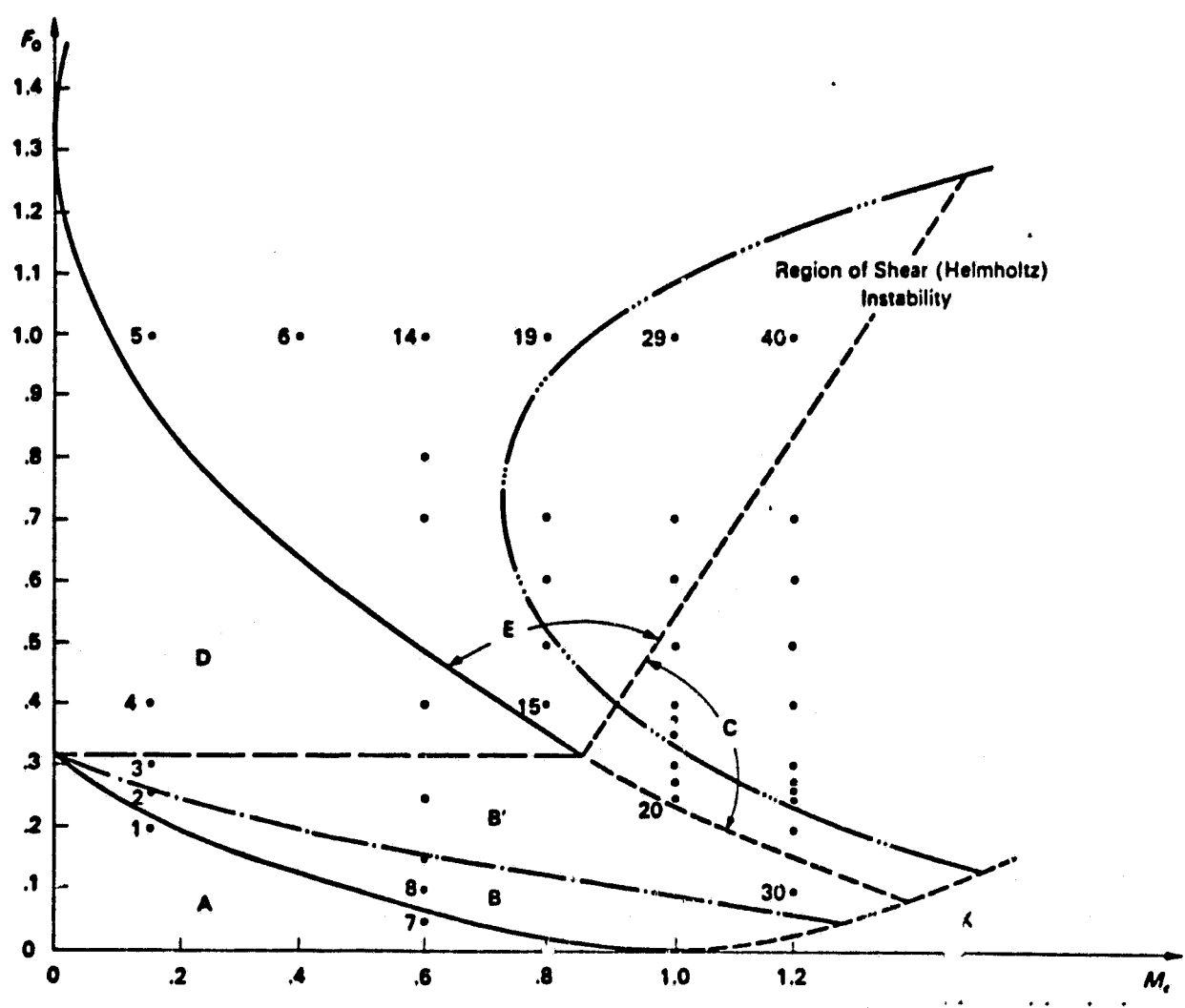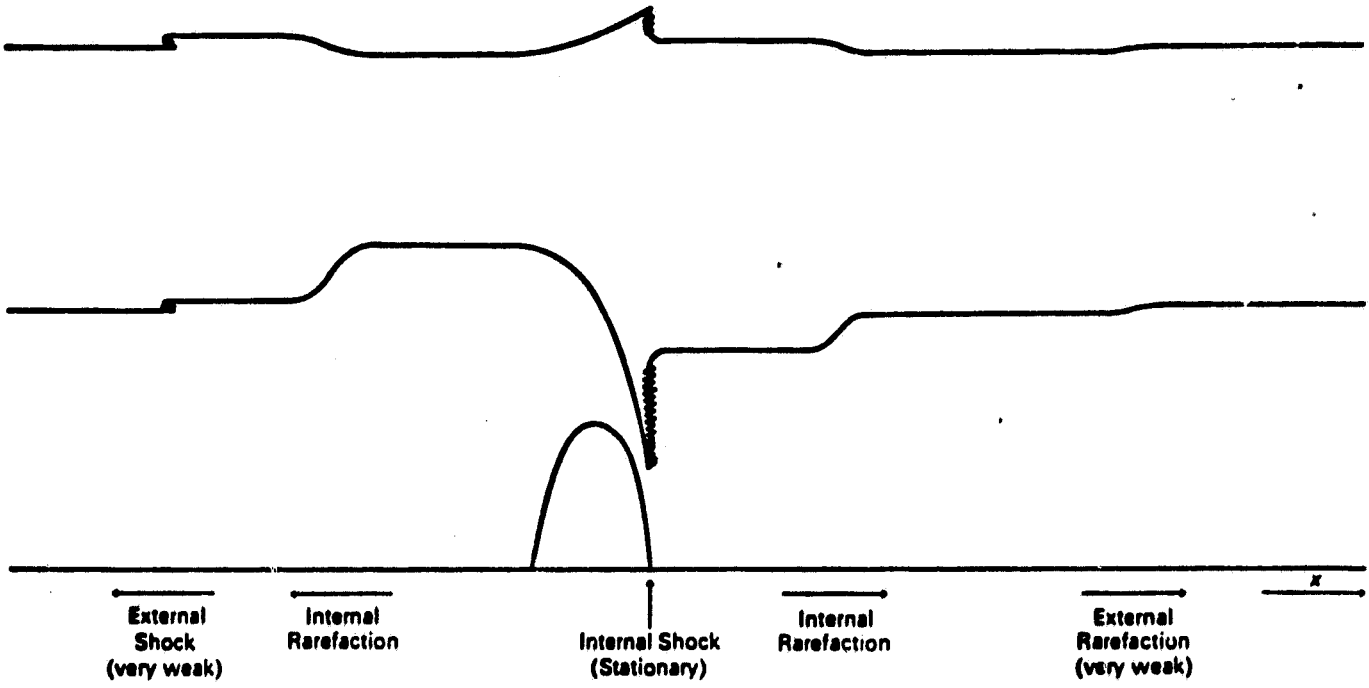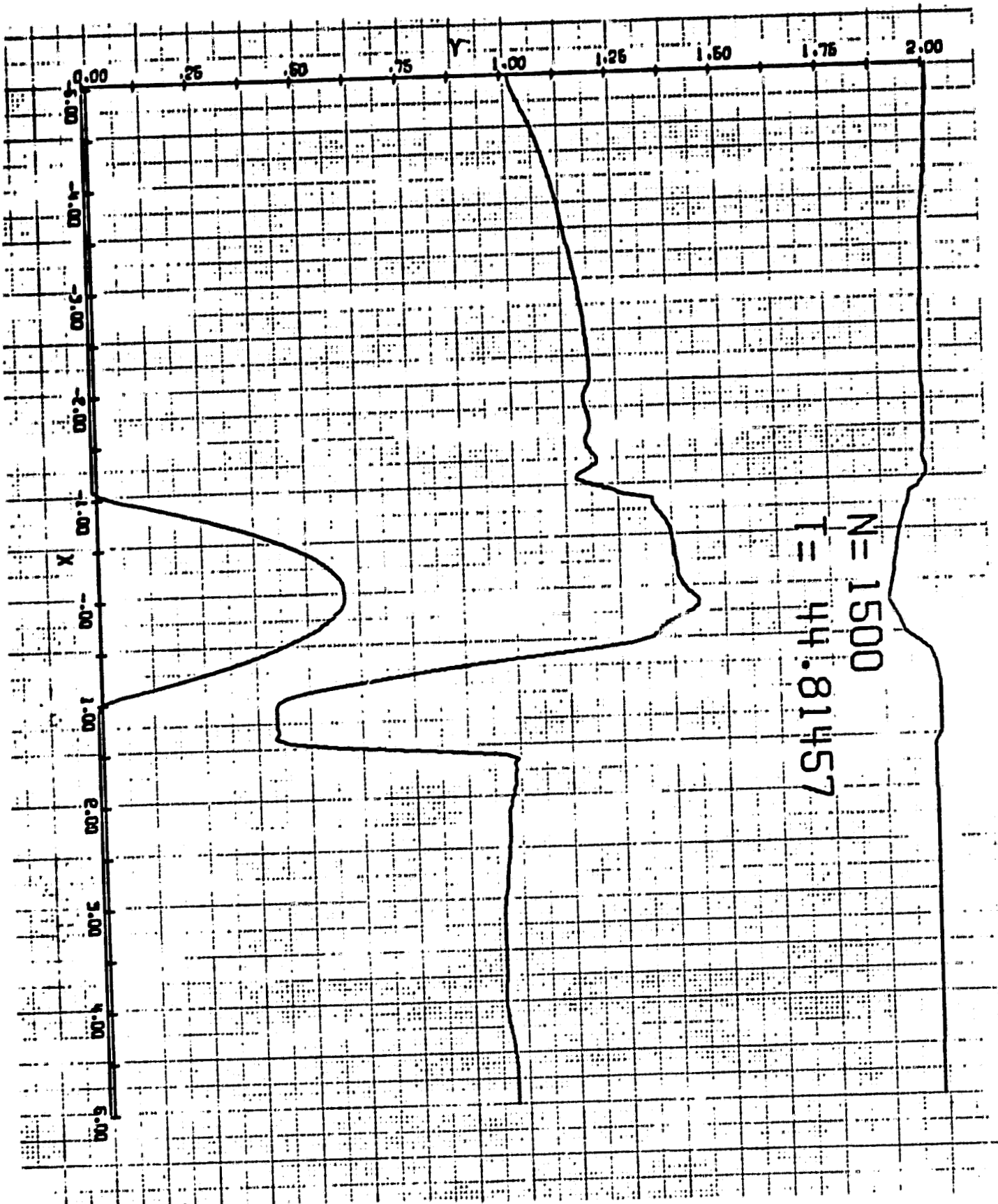   about 5 hours and 25 minutes after the initial time.

FIG 1

Layer 2
Density = ρ_1, $\frac{\rho_1}{\rho} = r$

Layer 1
Density = ρ

FIG 2

Region of Shear (Helmholtz) Instability

FIG 3

Region B

| External Shock (very weak) | Internal Rarefaction | Internal Shock (Stationary) | Internal Rarefaction | External Rarefaction (very weak) |

N= 1500
T= 44.81457

FIG 4a

FIG4b]

N=1750
T=52.26184

fig 5

N=1750

52.26765

X

Y
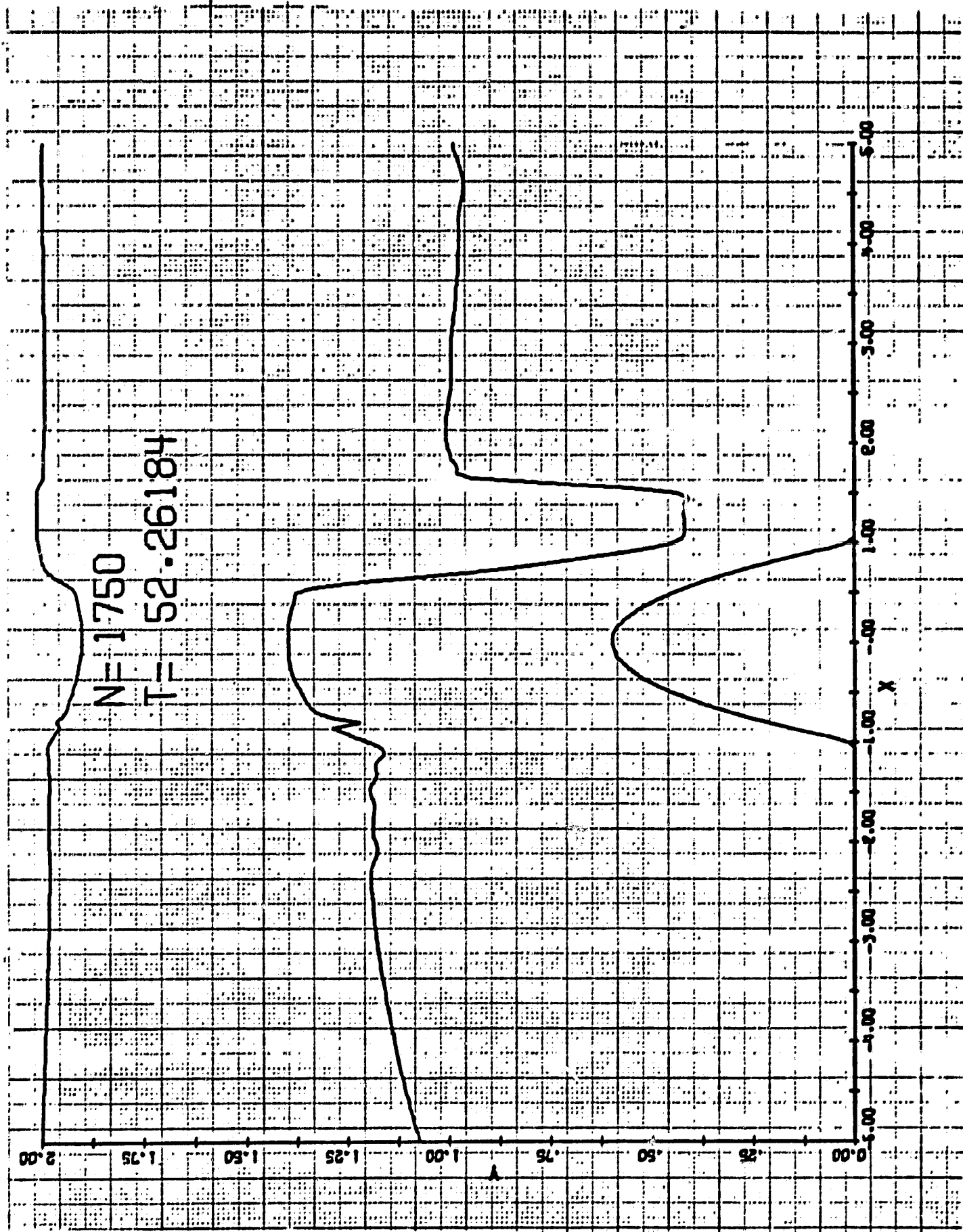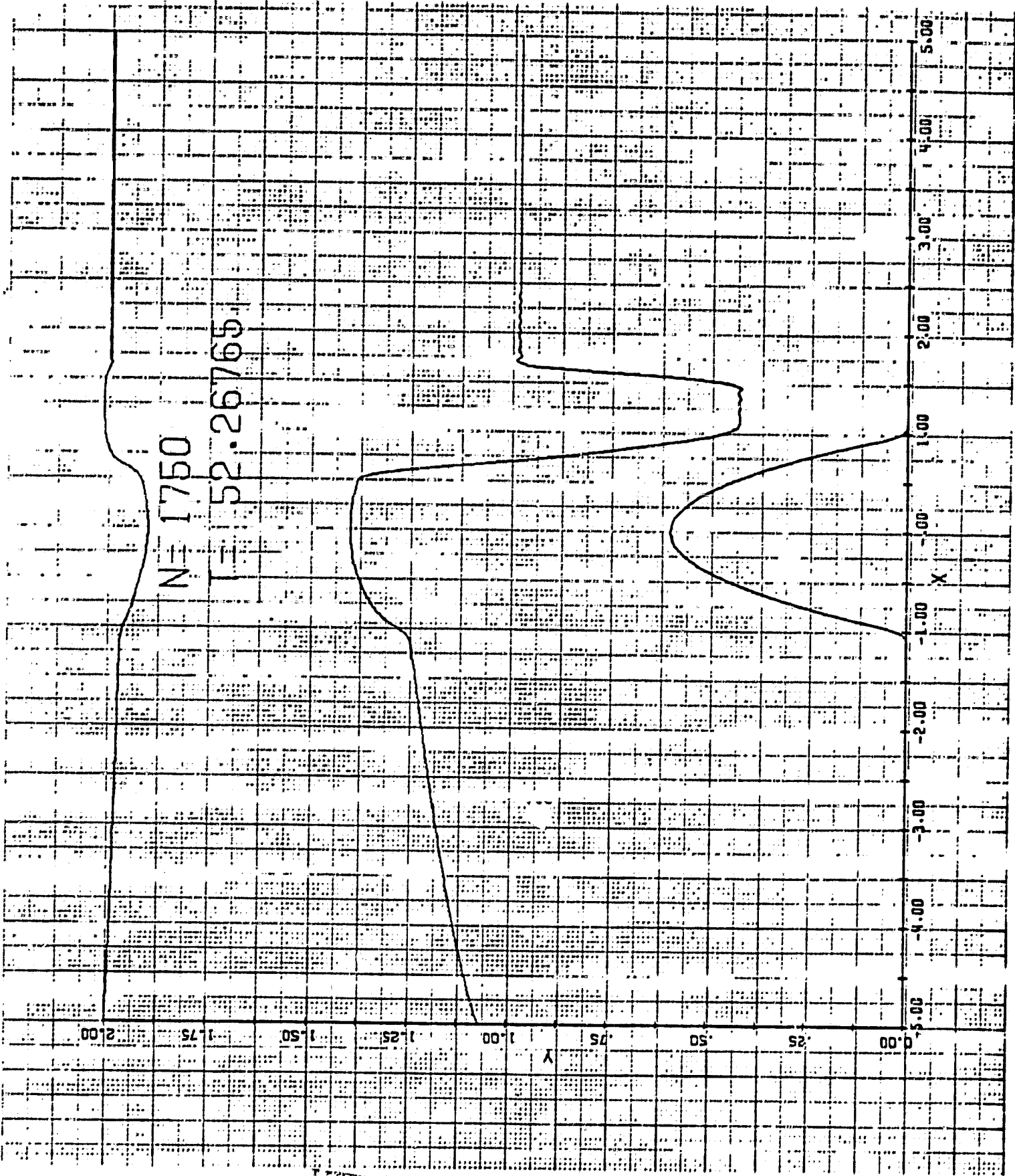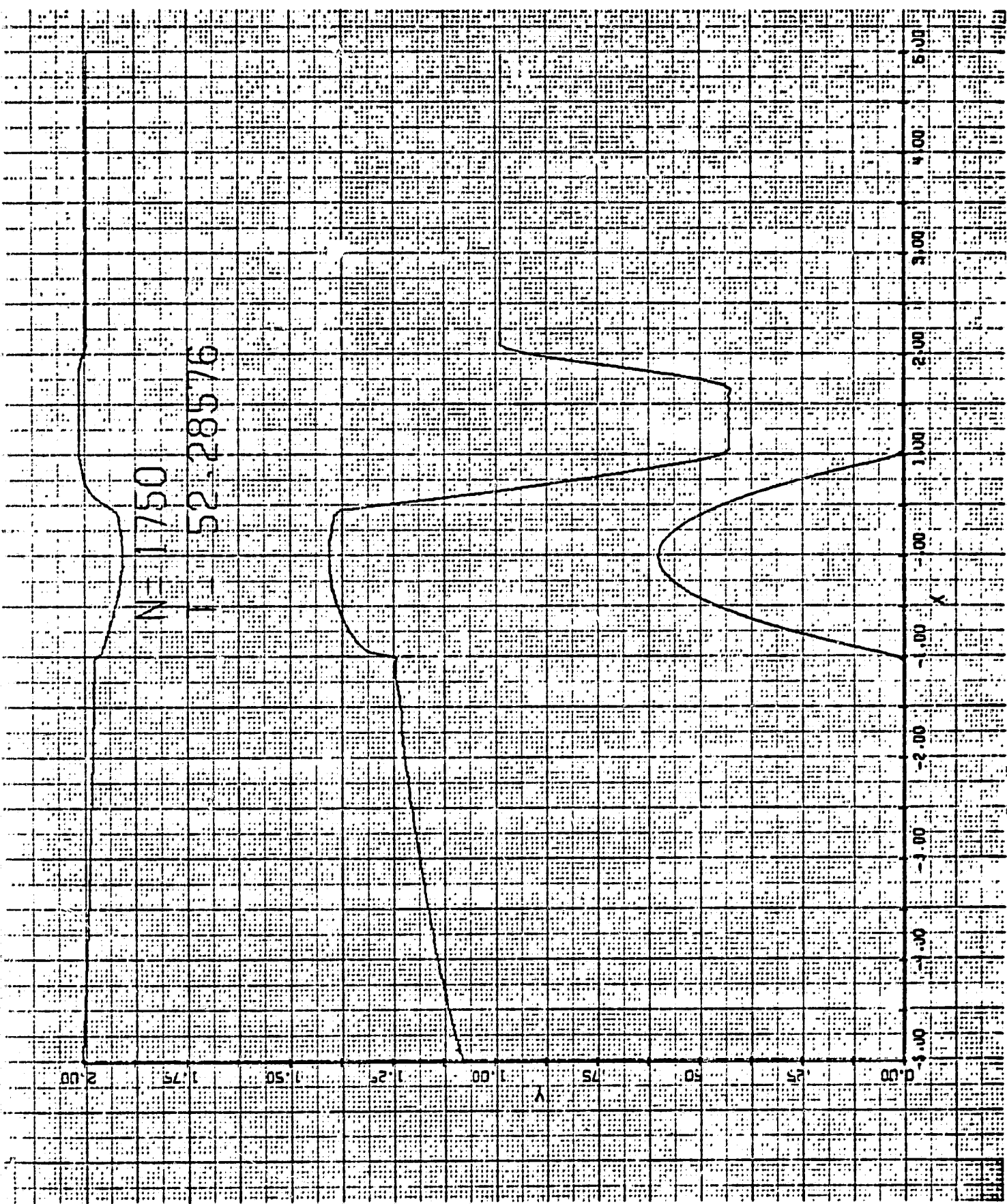
5.00 4.00 3.00 2.00 1.00 -1.00 -2.00 -3.00 -4.00 -5.00

2.00 1.75 1.50 1.25 1.00 .75 .50 .25 0.00

FIG 6

N = 1750
I = 52.28576

FIG 7

N = 1750
T = 52.2801

FIG 31

N= 3750
T= 47.13895